Continuous Flow Aerobic Oxidation of Benzyl Alcohol on Ru/Al$_2$O$_3$ Catalyst in a Flat Membrane Microchannel Reactor: an Experimental and Modelling Study

Gaowei Wu,[a] Enhong Cao,[a] Peter Ellis,[b] Achilleas Constantinou,† [a] Simon Kuhn,[c]

Asterios Gavriilidis*[a]

[a] Department of Chemical Engineering, University College London, Torrington Place, London, WC1E 7JE, U.K.

[b] Johnson Matthey Technology Centre, Blount's Court, Sonning Common, Reading, RG4 9NH, U.K.

[c] Department of Chemical Engineering, KU Leuven, Celestijnenlaan 200F, 3001 Leuven, Belgium

Corresponding Author: *E-mail: a.gavriilidis@ucl.ac.uk.

†Current address: Division of Chemical and Petroleum Engineering, School of Engineering, London South Bank University, 103, Borough Road, London SE1 0AA, U.K.

ABSTRACT

A flat Teflon AF-2400 membrane microchannel reactor was experimentally and theoretically investigated for aerobic oxidation of benzyl alcohol on 5 wt% Ru/Al_2O_3 catalyst. The flat membrane microchannel reactor consisted of gas and liquid channels (75 mm (L) × 3 mm (W) × 1 mm (D)), separated by a 0.07 mm thick semipermeable Teflon AF-2400 flat membrane, which allowed continuous supply of oxygen during the reaction and simultaneously avoided direct mixing of gaseous oxygen with organic reactants. A stability test was first carried out, and the experimental data obtained from the stabilization period were used to estimate the kinetics of benzyl alcohol oxidation with a 2D reactor model. Using the estimated kinetics, the modelling results obtained from the 2D reactor model agreed well with the experimental data at different liquid flow rates and oxygen pressures. The mass transfer and catalytic reaction in the membrane microchannel reactor were then theoretically studied by changing the membrane thickness, the liquid channel depth, and the reaction rate coefficient. Oxygen transverse mass transfer in the catalyst bed was found to be the controlling process, and decreasing the liquid channel depth is suggested to improve the oxygen supply and enhance the benzyl alcohol conversion in the membrane reactor.

1. Introduction

The high demand for sustainable processes has driven researchers in both academia and industry to employ solid catalysts and molecular oxygen rather than traditional, toxic chemical oxidants (Davis et al., 2013; Mallat and Baiker, 2004). However, aerobic oxidation of alcohols on solid catalysts is still hindered by several issues, such as lack of catalysts with sufficient activity and stability, and complex mass transport processes and reaction mechanisms (Gemoets et al., 2016). Moreover, potential safety risks in conventional batch or semi-batch reactors with oxidant-organic reactant mixtures are another particular challenge, since such reactions are generally exothermic and performed at elevated temperatures and pressures (Gavriilidis et al., 2016; Gemoets et al., 2016; Hone et al., 2017; Pieber and Kappe, 2016).

With the development of microreaction technology, microchannel reactors provide an excellent opportunity to address the above issues, and a variety of gas-liquid and gas-liquid-solid microchannel reactors has been developed so far (Elvira et al., 2013; Gutmann et al., 2015; Hessel et al., 2005; Jähnisch et al., 2004; Mallia and Baxendale, 2015). Among these, membrane microchannel reactors are an emerging type of reactors for process intensification, which combine the benefits of both membrane reactors and microchannel reactors (Aran et al., 2011a; Aran et al., 2011b; Hogg et al., 2012; Liu et al., 2016; Noël and Hessel, 2013; Selinsek et al., 2016; Tan and Li, 2013). The integration of membrane into a microchannel reactor forces gas and liquid phases to flow separately with a well-defined contacting interface. This allows better control of gas dosing and avoids direct mixing of gas and liquid. Simultaneously, the high surface-area-to-volume ratio in microchannel reactors could also contribute to the enhanced heat and mass transfer. These advantages make membrane microchannel reactors highly promising for intrinsically safe operation of aerobic alcohol oxidation.

As for the choice of available membranes, Teflon AF-2400 membrane has gained popularity, since it uniquely combines excellent chemical resistance, thermal stability, and mechanical properties with high fractional free volume (Zhang and Weber, 2012). Its distinctive permeabilities to gas and liquid also assure high flux of gas and low pervaporation of liquid through the membrane. The Ley group first developed a Teflon AF-2400 tube-in-tube membrane microreactor and applied it to key C-C, C-N, and C-O bond forming and hydrogenation reactions (Brzozowski et al., 2015). In our previous work, Au-Pd/TiO$_2$ catalyst particles were directly packed in a tube-in-tube membrane microreactor and used for aerobic oxidation of benzyl alcohol (Wu et al., 2015). The continuous supply of oxygen through the membrane during the reaction contributed to significantly improved conversion and selectivity as compared to a reactor operating with an oxygen pre-saturated feed. However, the performance of the membrane microreactor still lacks deep understanding, due to the complex reaction kinetics of benzyl alcohol oxidation on Au-Pd/TiO$_2$ catalysts. More recently, a scalable flat membrane reactor implemented with a Teflon AF-2400 membrane and porous carbon cloth was demonstrated for heterogeneous Pd-catalyzed hydrogenations and homogenous Cu(I)/TEMPO alcohol oxidations (Mo et al., 2018).

Ru-based catalysts have been investigated for oxidation of alcohols, featuring low activity but high selectivity (Davis et al., 2013; Yamaguchi and Mizuno, 2002). The selectivity to benzaldehyde in oxidation of benzyl alcohol on Ru-based catalyst is commonly reported to be >99% under moderate reaction conditions (Mannel et al., 2014; Yamaguchi and Mizuno, 2002; Yang et al., 2015). In this study, a flat AF-2400 membrane microchannel reactor was experimentally and theoretically investigated for aerobic oxidation of benzyl alcohol with Ru/Al$_2$O$_3$ catalyst. The stability of the Ru/Al$_2$O$_3$ catalyst was studied and the kinetics of the benzyl alcohol oxidation was evaluated with a 2D reactor model, in an attempt to better

understand the mass transfer and catalytic reactions in the reactor and provide guidance for its improvement.

2. Experimental Section

2.1 Catalyst preparation

Ruthenium chloride (Johnson Matthey, 40.34% Ru), sodium hydroxide (Alfa Aesar) and gamma-aluminium oxide (γ-Al_2O_3, Sasol HP14-150) were all used as received. The 5 wt% Ru/Al_2O_3 catalyst was prepared by deposition-precipitation. The γ-Al_2O_3 support was suspended in water at 338 K to form a slurry. To this slurry, two solutions were added: 0.03 M NaOH and 0.05 M $RuCl_3$. The pH of the slurry was maintained at pH 9 by addition of appropriate amounts of these two solutions. Once addition of the ruthenium salt was complete, the temperature of the slurry was raised to boiling, and was then allowed to cool. The catalyst was separated by filtration, and the filtrate was washed thoroughly with hot water. Finally, the catalyst was dried at 373 K overnight. The ruthenium content was analysed by Inductively Coupled Plasma (ICP) analysis and found to be 4.46 wt% Ru. The powder was pelletized, crushed, and sieved to the desired particle size range (90-125 μm). The physical properties of the catalyst particles were characterized with QUADRASORB evo^{TM} 4 BET Stations and Pentapyc^{TM} 5200e Gas Pycnometer. The surface area was found to be 142 m^3/g, the pore radius 8.1 nm and pore volume 0.72 cm^3/g. The skeletal density of the catalyst was 3.38 g/cm^3, from which the catalyst porosity was calculated to be 0.71.

2.2 Flat membrane microchannel reactor set-up

As shown in Figure 1, the reactor consists of liquid and gas flow plates machined in 316 stainless steel (channel size length: 75 mm; width: 3 mm; depth: 1 mm), between which a Teflon AF-2400 membrane (length: 85 mm; width: 30 mm; thickness: 0.07 mm; Biogeneral),

a 304 stainless steel mesh (length: 85 mm; width: 30 mm; thickness: 0.05 mm; hole size: 76 μm; open area: 23%; Industrial Netting), gasket (length: 85 mm; width: 30 mm; thickness: 1 mm; open area length: 75 mm; width: 3 mm; Altec) were assembled. An O-ring groove was machined in the liquid flow plate, which allowed other meshes (e.g. sintered metal) also to be used as the membrane support. Catalyst particles (particle size: 90-125 μm; 100 mg) were retained at the end of the liquid channel by a small circular piece of another nickel mesh (diameter: ~2 mm; thickness: 0.05 mm; hole size: 25μm; Tecan). The length of the catalyst bed in the liquid channel was measured to be ~5 cm. Hence, the void fraction of the catalyst bed was estimated to be 0.32.
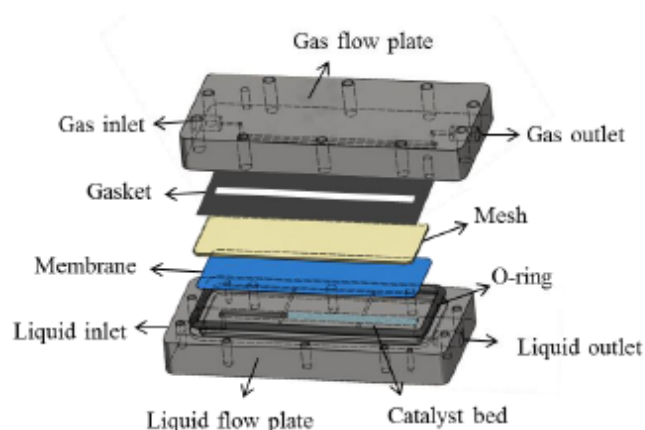

Figure 1. Schematic of the flat membrane microchannel reactor consisting of gas and liquid flow plates with viton gasket, stainless steel mesh, and Teflon AF-2400 membrane

The reactor was heated with a hotplate (Gallenkamp) fitted with a thermocouple, and the actual temperature inside the reactor was measured through the inserted thermocouples (1 mm away from the liquid channel). To decrease heat loss, an insulation cap (insulation thickness: ~2 cm; WDS® Ultra, Morgan) was made to cover the reactor. The temperature differences between the gas and the liquid flow plates during the reaction at 373 K were measured to be less than 3 K.

Neat benzyl alcohol (1-10 µL/min, 99.0%, Sigma-Aldrich) was delivered into the reactor with a HPLC pump (Knauer P2.1S). The pressure of the liquid was controlled with an adjustable back pressure regulator (BPR, Zaiput, BPR-01) and measured by a pressure sensor (Zaiput, Hastelloy/PFA wetted parts). Pure oxygen (BOC, grade N6.0), 5 mL/min (at standard temperature and pressure), regulated by a mass flow controller (Brooks, GF40 series)) was directed to the gas channel to ensure the organic vapour concentration in the gas phase was lower than 1 vol% (the lower explosive limit for toluene in air at 6 bara and 393 K (Goethals et al., 1999); data on benzyl alcohol were not available). The pervaporation of benzyl alcohol and benzaldehyde through the Teflon AF-2400 membrane was experimentally measured and presented in the Supporting Information. A BPR (Swagelok, K series) was connected at the gas outlet to maintain the desired gas pressure. The actual gas pressure was monitored by a pressure sensor (Zaiput, Hastelloy/PFA wetted parts). The effluent from the liquid outlet was collected in a 2 mL vial (placed in an ice-water cold trap) and quantitatively analysed by a gas chromatograph (Agilent 7820A) fitted with a DB-624 capillary column and a flame ionization detector. For each set of experiment, at least three samples were collected and the results were averaged. The errors for the conversion and benzaldehyde selectivity were less than ±2 %.

Benzyl alcohol conversion (X) and selectivity (S_B) to benzaldehyde were calculated according to the following equations:

$$X = \frac{c_{BnOH,in} - c_{BnOH,in}}{c_{BnOH,in}} \times 100\% \qquad (1)$$

$$S_B = \frac{c_B}{c_{BnOH,in} \cdot X} \times 100\% \qquad (2)$$

where $c_{BnOH,in}$ and $c_{BnOH,out}$ are the concentration of benzyl alcohol at the reactor inlet and outlet, respectively. c_B is the concentration of benzaldehyde at the outlet.

Catalyst contact time (*CCT*) was used to characterise the reaction time of benzyl alcohol, and was defined as

$$CCT = \frac{m_{cat}}{v \cdot \rho} \tag{3}$$

where m_{cat} is the mass of catalyst , v is the volumetric flow rate of benzyl alcohol at the inlet, ρ is the density of benzyl alcohol.

Turnover frequency (*TOF*) was calculated to quantitatively represent the reaction rate

$$TOF = \frac{F_{BnOH} \cdot X}{n_{Ru}} \tag{4}$$

where F_{BnOH} is the molar flow rate of benzyl alcohol at the inlet and n_{Ru} is the moles of Ru contained in the catalyst bed.

3. Mathematical Model

A 2D reactor model was developed to simulate the mass transfer and catalytic reaction in the reactor based on the following assumptions: 1) steady-state and isothermal conditions; 2) Henry's law applies at the membrane-liquid interface; 3) ideal gas behavior is valid for the gas phase; 4) uniform axial fluid velocity in the liquid phase with constant physical properties and transport coefficients; 5) negligible dissolution of liquid in the membrane and pervaporation to the gas phase; 6) negligible pressure drop along the catalyst bed (the pressure drop was measured to be less than 0.1 bara during the experiment). Since the oxygen pressure in the gas phase was constant at given oxygen pressure, only the liquid channel and membrane were considered with boundary condition of constant oxygen concentration at the interface of gas and membrane.
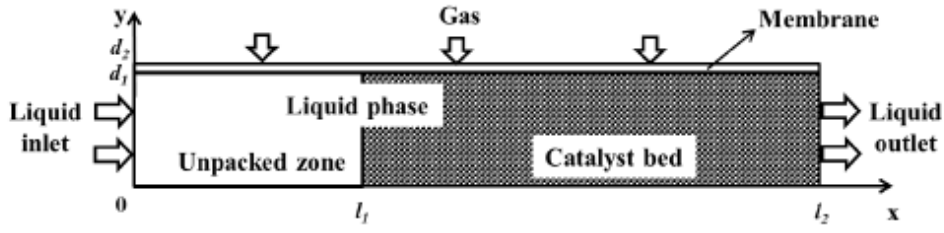
Figure 2. Membrane reactor model used for the simulations (not to scale)

3.1 Mass balance in the reactor

The simulation of the liquid phase was realized through multiscale coupling of the catalyst particles with the bulk liquid phase. The continuity equation for species in the unpacked zone can be expressed as:

$$u_x \frac{\partial c_i}{\partial x} = D_i \left(\frac{\partial^2 c_i}{\partial x^2} + \frac{\partial^2 c_i}{\partial y^2} \right) \tag{5}$$

where i stands for oxygen or benzyl alcohol, c_i is the concentration of i in the bulk liquid phase, D_i is the molecular diffusion coefficient in the bulk liquid, u_x is the liquid velocity in the axial direction.

The continuity equation for species in the catalyst bed is

$$u_x \frac{\partial c_i}{\partial x} = D_{i,A} \frac{\partial^2 c_i}{\partial x^2} + D_{i,T} \frac{\partial^2 c_i}{\partial y^2} - J_i A_b \tag{6}$$

where $D_{i,A}$ is the axial dispersion coefficient, $D_{i,T}$ is the transverse dispersion coefficient, J_i is the molar flux of i into the catalyst particles, A_b is the specific surface area exposed to the liquid of the packed bed, assuming randomly packed spherical particles (Richardson et al., 2002).

$$A_b = \frac{3}{r_p} (1 - \varepsilon_b) \tag{7}$$

where r_p is the average radius of catalyst particles, and ε_b is the catalyst bed void fraction.

The external mass transfer resistance is expressed in terms of mass transfer coefficient

$$J_i = h_i(c_i - c_{i,ps}) \tag{8}$$

$$h_i = \frac{Sh \cdot D_i}{2r_p} \tag{9}$$

$$Sh = 2 + 0.552Re^{1/2}Sc^{1/3} \tag{10}$$

$$Sc = \frac{\mu}{\rho \cdot D_i} \tag{11}$$

$$Re = \frac{2r_p \cdot \rho \cdot u_x}{\mu} \tag{12}$$

where $c_{i,ps}$ is the concentration of i at the catalyst particle surface, h_i is the external mass transfer coefficient. Sh is the Sherwood number, which is calculated using the Frössling correlation (Froessling, 1938). Sc is the Schmidt number, μ is viscosity of benzyl alcohol, ρ is the density of benzyl alcohol, Re is the particle Reynolds number.

The simulation of the reaction inside the catalyst particles was realized in COMSOL® using the Reaction Pellet Bed feature. This feature has a predefined extra dimension (1D) on the dimensionless catalyst particle radius ($r = r_{dim}/r_p$, r_{dim} is the spatial radial coordinate in the particle) of the catalyst particle. The mass balance inside the catalyst particles is derived from a shell balance across a spherical shell

$$\frac{\partial}{\partial r}(r^2 D_{i,eff}\frac{\partial c_{i,p}}{\partial r}) = r^2 r_p^2 R_{i,p} \tag{13}$$

where r is a dimensionless catalyst particle radius, $D_{i,eff}$ is the effective diffusion coefficient of i in the catalyst pores, $c_{i,p}$ is the concentration of i in the catalyst particle, $R_{i,p}$ is the reaction rate per unit volume of catalyst particle.

For Ru/Al$_2$O$_3$ catalyzed aerobic oxidation of benzyl alcohol, the amount of oxygen consumed was observed to be half of the benzyl alcohol consumed, with a benzaldehyde selectivity > 99% (Yamaguchi and Mizuno, 2003). So, the overall reaction is

$$PhCH_2OH + 1/2\,O_2 \rightarrow PhCHO + H_2O \tag{14}$$
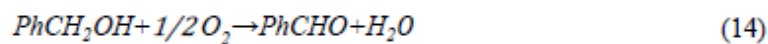
and the kinetics of the oxidation reaction was modeled as a α-order reaction in benzyl alcohol and a β-order reaction in oxygen

$$R_{BnOH,p} = -kc_{BnOH,p}^{\alpha} c_{O2,p}^{\beta} \tag{15}$$

$$R_{O2,p} = -\frac{1}{2}kc_{BnOH,p}^{\alpha} c_{O2,p}^{\beta} \tag{16}$$

where $R_{BnOH,p}$ and $R_{O2,p}$ are the reaction rate of benzyl alcohol and oxygen in the catalyst particle, k is the reaction rate coefficient, which is estimated based on the experimental results.

Boundary conditions used were:

$$at\ x = 0, \quad c_{BnOH} = c_{BnOH,in}, \quad c_{O2} = 0 \tag{17}$$

$$at\ x = l_2, \quad \frac{\partial c_i}{\partial x} = 0 \tag{18}$$

$$at\ y = 0, \quad \frac{\partial c_i}{\partial y} = 0 \tag{19}$$

$$at\ y = d_1, \quad c_{O2} = \frac{c_{O2,m}}{H}, \quad \frac{\partial c_{BnOH}}{\partial y} = 0 \tag{20}$$

$$at\ r = 1, \quad c_{i,p} = c_{i,ps} \tag{21}$$

$$at\ r = 0, \quad \frac{\partial c_{i,p}}{\partial r} = 0 \tag{22}$$

where $c_{BnOH,in}$ is the inlet concentration of benzyl alcohol, $c_{O2,m}$ is the oxygen concentration in the membrane, H is the dimensionless Henry solubility of oxygen in benzyl alcohol at 373 K. Reactant conversion was calculated based on the average concentration of benzyl alcohol at the outlet.

3.2 Mass balance in the membrane

The steady-state mass balance for oxygen transfer in the membrane, which is considered to be by diffusion alone, can be expressed as:

$$D_{O2,m}\left(\frac{\partial^2 c_{O2,m}}{\partial x^2} + \frac{\partial^2 c_{O2,m}}{\partial y^2}\right) = 0 \tag{23}$$

where $c_{O2,m}$ is the oxygen concentration in the membrane, which is essentially the oxygen concentration in thermal equilibrium with the membrane. $D_{O2,m}$ is an oxygen diffusion coefficient in the membrane obtained from the membrane permeability (Yang and Jensen, 2013).

Boundary conditions:

$$at \ y = d_1, \quad c_{o2,m} = Hc_{o2} \tag{24}$$

$$at \ y = d_2, \quad c_{o2,m} = c_{o2,g} \tag{25}$$

where $c_{O2,g}$ is the oxygen concentration in the gas phase.

The mass balance equations together with the boundary conditions were solved using COMSOL Multiphysics software version 5.2a. A mesh consisting of 33,000 elements and 530,007 degree of freedom was used and the results were found to be mesh independent. The values of the variables used in the model are shown in Table 1 and the calculation details are shown in the Supporting Information.

Table 1. List of parameter values used in the model

Symbol	Value	Units	Description
$c_{O2,g}$	$\dfrac{P_{O2}}{\overline{R}T}$	mol/m^3	Oxygen concentration in the gas phase
$c_{BnOH,in}$	9621	mol/m^3	Benzyl alcohol inlet concentration
d_1	1.00	mm	Reactor liquid channel depth
d_2	1.07	mm	Reactor liquid channel depth and membrane thickness
D_{BnOH}	2.01×10^{-9}	m^2/s	Diffusion coefficient of benzyl alcohol in the bulk liquid at 373 K (Hayduk and Buckley, 1972; Reddy and Doraiswamy, 1967)
D_{O2}	5.19×10^{-9}	m^2/s	Diffusion coefficient of O_2 in benzyl alcohol at 373 K (Hayduk and Buckley, 1972; Wilke and Chang, 1955)
$D_{BnOH,A}$	0.46×10^{-9}	m^2/s	Axial dispersion coefficient of benzyl alcohol (Delgado, 2006)
$D_{BnOH,T}$	0.46×10^{-9}	m^2/s	Transverse dispersion coefficient of benzyl alcohol (Delgado, 2006)

$D_{O2,A}$	1.19×10^{-9}	m²/s	Axial dispersion coefficient of oxygen (Delgado, 2006)
$D_{O2,T}$	1.19×10^{-9}	m²/s	Transverse dispersion coefficient of oxygen (Delgado, 2006)
$D_{BnOH,eff}$	1.01×10^{-9}	m²/s	Effective diffusion coefficient of benzyl alcohol in the catalyst particle (Froment et al., 2010)
$D_{O2,eff}$	2.62×10^{-9}	m²/s	Effective diffusion coefficient of oxygen in the catalyst particle (Froment et al., 2010)
$D_{O2,m}$	1.19×10^{-9}	m²/s	Diffusion coefficient of oxygen in the membrane at 373K based on oxygen concentration in the gas phase (Yang and Jensen, 2013; Zhang and Weber, 2012)
H	9.9	-	Dimensionless Henry solubility of oxygen in benzyl alcohol at 373 K (Wu et al., 2017)
l_1	25	mm	Length of the unpacked zone in the liquid channel
l_2	50	mm	Length of the catalyst bed
M_{BnOH}	108.1	g/mol	Molecular weight of benzyl alcohol
P_{O2}	1-8	bara	Oxygen pressure in the gas phase
r_p	54	μm	Average radius of catalyst particles
$\bar{R}$	8.314×10^{-9}	m³·bar/(K·mol)	Ideal gas constant
u_x	$\dfrac{v}{wd_1}$	cm/s	Axial liquid superficial velocity vector
w	3	mm	Liquid channel width
ε_p	0.71	-	Catalyst particle porosity
ε_b	0.32	-	Catalyst bed void fraction
μ	7.49×10^{-4}	Pa·s	Viscosity of benzyl alcohol at 373 K (Yaws, 2014)
ρ	1.0	g/mL	Density of benzyl alcohol at 373 K (Nayar and Kudchadker, 1973)
v	1-10	μL/min	Liquid flow rate at the inlet

4. Results and Discussion
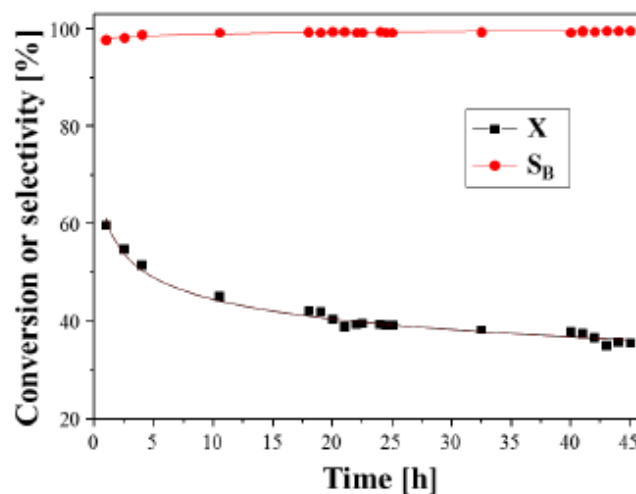
4.1 Stability of Ru/Al₂O₃ catalyst

Figure 3. Stability study of the Ru/Al$_2$O$_3$ catalyst in aerobic oxidation of benzyl alcohol. Conversion and selectivities are shown as a function of operation time. Reaction conditions: Ru/Al$_2$O$_3$ catalyst (90-125 μm), 100 mg; neat benzyl alcohol, 2 μL/min; catalyst contact time, 48 g$_{cat}$·min/g$_{BnOH}$; oxygen pressure, 8.0 bara; liquid pressure, 9.0 bara; reaction temperature, 373 K. X, conversion of benzyl alcohol; S$_B$, selectivity to benzaldehyde.

Initially, the performance of the Ru/Al$_2$O$_3$ catalyst was experimentally evaluated in the flat membrane microchannel reactor, and the results are shown in Figure 3. A fast deactivation process was observed in the first ~ 20 h. Only 5% conversion drop was observed in the following 25 h. Mannel et al. (2014) also observed a fast deactivation rate followed by a slower one in a catalyst packed stainless steel tube reactor, which was attributed to poisoning of active sites by benzoic acid. Brazier et al. (2017) further derived an equation for the effect of oxygen on Ru/Al$_2$O$_3$ catalyst deactivation, which accounted for a fast and reversible inhibition by the formed benzoic acid, combined with a slower and irreversible loss of active sites caused by Ru reduction. Since the selectivity to benzaldehyde stabilized at 99% within the 45 h, 100% selectivity to benzaldehyde was assumed in the model without considering any other minor by-products.

For the reaction kinetics, Yamaguchi and Mizuno (2003) studied the kinetics and mechanism of alcohol oxidation on Ru/Al$_2$O$_3$ catalyst in a batch reactor. The reaction rate

was found to be of fractional order with the benzyl alcohol (first-order at low concentrations and zero-order at high concentrations; alcohol concentration range: 0-2 M) and a zero order on the oxygen pressure (0.2-3.0 bar). Using a multichannel packed bed reactor, Bavykin et al. (2005) observed that the yield of benzaldehyde in oxidation of benzyl alcohol (1 M) on Ru/Al_2O_3 catalyst was affected by the oxygen pressure at pressure lower than 9 bara and was independent of the oxygen pressure at pressures above 9 bara. Zotova et al. (2010) studied aerobic oxidation of alcohols to aldehydes and ketones on Ru/Al_2O_3 catalyst in a commercially-available XCube^{TM} reactor by pre-mixing and saturating the liquid with the gaseous reactant before reaching the catalyst bed. The oxidation of benzyl alcohol was indicated to be a pseudo-first-order with respect to benzyl alcohol (up to 0.2 M), and oxygen was found to be integral to the kinetics of the reaction, since the reaction rate was significantly enhanced by increasing the oxygen pressure from 6 to 26 bara. In a following study, the reaction rate was re-examined in a plug flow differential reactor with an inline FTIR, and was found to be of zero order with benzyl alcohol (0.1 M) under reaction conditions not subject to mass transfer limitations, and a partial positive order in oxygen (oxygen saturation pressure up to 26 bara) (Brazier et al., 2017). The different observed kinetics was probably caused by the different ratios of oxygen concentration to benzyl alcohol concentration in different types of reactors.

The focus of this study is to understand the mass transfer and catalytic reaction interaction and membrane reactor behaviour, and thus a detailed kinetic study of benzyl alcohol oxidation on Ru/Al_2O_3 catalyst was not pursued. Since the oxygen concentration varied axially and transversely in the catalyst bed, resulting in varied ratios of oxygen to benzyl alcohol concentration, a reaction rate assuming a first order in benzyl alcohol and a 0.5 order in oxygen was used in the modelling ($\alpha = 1$ and $\beta = 0.5$ used in eqn.15&16). The average conversion at the stable period in Figure 3 (40%, 20-40 h) was used to estimate the

corresponding reaction rate coefficient (k), which made the modelling conversion equal to the experimental value under the same reaction conditions. The estimated k was 3.9×10^{-4} $m^{3/2}/(mol^{1/2} \cdot s)$, which was then used for the reaction rate under other reaction conditions (e.g. different liquid flow rates and oxygen pressures).
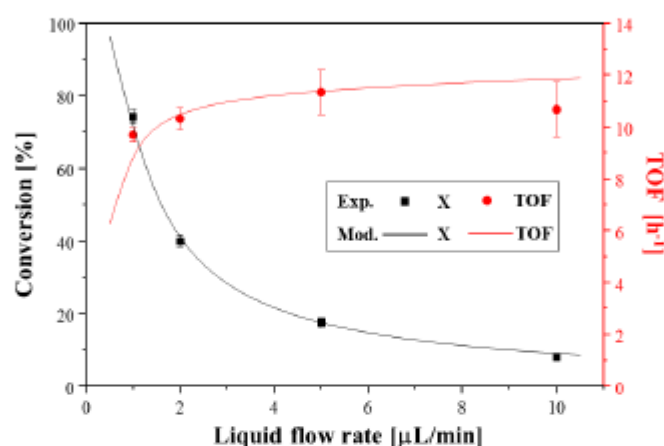
4.2 Effect of liquid flow rate

Figure 4. Effect of liquid flow rate on the conversion of benzyl alcohol and TOF, obtained from experiment and modelling. Reaction conditions: Ru/Al_2O_3 catalyst (90-125 μm), 100 mg; neat benzyl alcohol; oxygen pressure, 8 bara; liquid pressure, 9.0 bara; reaction temperature, 373 K.

The effect of liquid flow rate on the conversion of benzyl alcohol was modelled under the same oxygen pressure (8 bara), and the modelling results are compared with the experimental values in Figure 4. Good agreement was observed between the modelling and the experimental results under different liquid flow rates. Since the reaction rate was estimated only based on results under liquid flow rate of 2 μL/min, the good agreement shows that the model based on the estimated kinetics provided satisfactory prediction of reactor performance.

In Figure 4, high conversion was obtained at low liquid flow rate. Since the length of catalyst bed was constant (due to the same amount of catalyst), the enhanced conversion was due to the longer time for oxygen permeation and reaction (Constantinou et al., 2015; Wu et

al., 2015). Theoretically, full conversion of benzyl alcohol could be achieved at liquid flow rate of ~0.4 µL/min. This corresponds to a catalyst contact time of 240 $g_{cat} \cdot min/g_{BnOH}$.

Average TOF was calculated to better compare the reaction rates at different liquid flow rates. From Figure 4, the profile of TOF was observed to increase dramatically with liquid flow rate increasing and then reach a plateau at liquid flow rate higher than 2 µL/min. Notably, the TOF was ~11 h^{-1} at liquid flow rate higher than 2 µL/min and 8 bara oxygen pressure, which corresponded to an oxygen consumption rate of 6.7×10^{-7} mol/($g_{cat} \cdot s$). These values are comparable to previous work where Ru/Al$_2$O$_3$ was used in a packed bed reactor with diluted oxygen (~6 h^{-1} at 353 K and 11 bar of 8% oxygen in nitrogen)(Mannel et al., 2014) or oxygen pre-saturated flow (13 h^{-1} at 373 K and 26 bara oxygen pre-saturation pressure) (Brazier et al., 2017), and a PTFE membrane reactor (2 h^{-1} at 353 K and 10.2 bar oxygen pressure) (Greene et al., 2015). However, the TOF observed in the membrane reactor is lower than those obtained in a batch reactor with bubbled oxygen (63 h^{-1} at 356 K and 1 bara) (Yamaguchi and Mizuno, 2002) and a multichannel packed bed reactor with high flow rate of pure oxygen (~110 h^{-1} at 375 K and 25 bara pressure) (Bavykin et al., 2005).
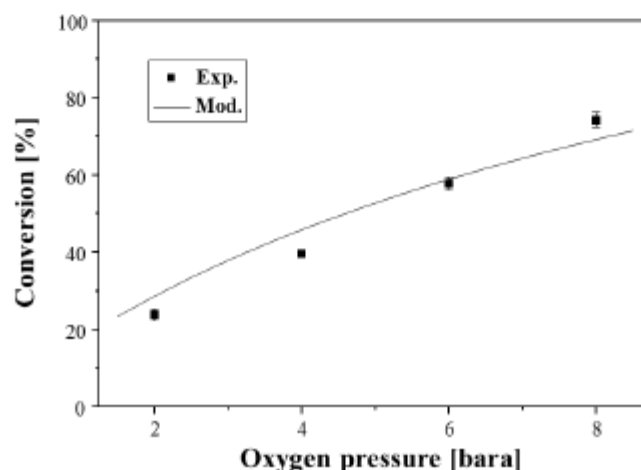
4.3 Effect of oxygen pressure

Figure 5. Effect of oxygen pressure on the conversion of benzyl alcohol, obtained from experiment and modelling. Reaction conditions: Ru/Al_2O_3 catalyst (90-125 µm), 100 mg; neat benzyl alcohol, 1 µL/min; catalyst contact time, 96 $g_{cat} \cdot min/g_{BnOH}$; liquid pressure, 1.0 bara higher than oxygen pressure; reaction temperature, 373 K.

Figure 5 presents the effect of oxygen pressure on the conversion of benzyl alcohol in the flat membrane microchannel reactor. Model prediction agrees well with the experimental results. The conversion of benzyl alcohol varied approximately linearly with the oxygen pressure and reached ~70% at 8 bara. A linear trend was also observed in the Teflon tube-in-shell membrane reactors with homogeneous Cu/TEMPO catalyst (Greene et al., 2015) and a Teflon AF-2400 tube-in-tube membrane reactor with heterogeneous Au-Pd/TiO₂ catalyst (Wu et al., 2015). Since the increase of oxygen pressure could increase the oxygen solubility in the liquid, the oxygen pressure-dependent conversion demonstrates that oxygen has a positive effect on the reaction rate under the conditions investigated. So, the lower TOF of Ru/Al_2O_3 catalyst in the membrane reactor as compared to those in a batch reactor (Yamaguchi and Mizuno, 2002) and a packed bed reactor with pure oxygen (Bavykin et al., 2005), was probably caused by the high loading of Ru in this study, as well as insufficient oxygen supply in the membrane reactor.
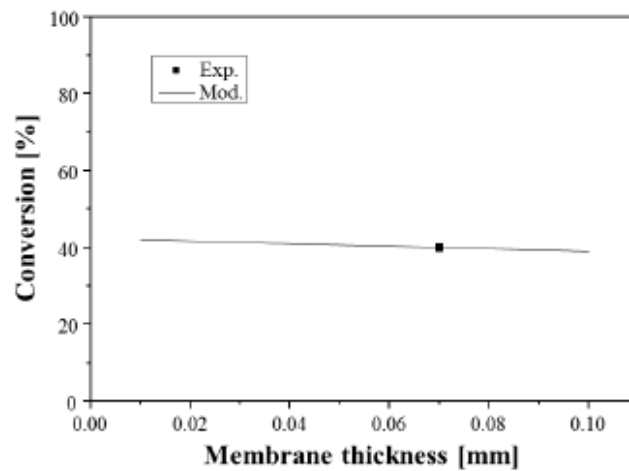
4.4 Effect of membrane thickness

Figure 6. Effect of membrane thickness on the conversion of benzyl alcohol, obtained from modelling. The square indicates experimental point. Reaction conditions: Ru/Al$_2$O$_3$ catalyst (90-125 µm), 100 mg; neat benzyl alcohol, 2 µL/min; catalyst contact time, 48 g$_{cat}$·min/g$_{BnOH}$; oxygen pressure, 8.0 bara; reaction temperature, 373 K.

Having now a validated membrane reactor model, we proceed to investigate the effect of various parameters in order to better understand reactor performance and provide guidance for its improvement. The effect of membrane thickness was studied using the model and the results are shown in Figure 6. Less than 4% increase in the conversion of benzyl alcohol was observed when decreasing the membrane thickness from 0.10 mm to 0.01 mm. These results indicate that the oxygen transfer resistance in the membrane has no significant effect on the reactor performance, probably due to the high permeability of the Teflon AF-2400 membrane. Indeed, the oxygen diffusion coefficient in the membrane ($D_{O2,m}$) was in the same order of magnitude as the oxygen transverse dispersion coefficient or the oxygen effective diffusion coefficient in the catalyst particles, but note that $D_{O2,m}$ was based on the oxygen concentration in the gas phase. To convert $D_{O2,m}$ to that based on the oxygen concentration in the liquid phase ($D'_{O2,m}$), which also made the oxygen concentration continuous across the membrane-liquid phase, $D_{O2,m}$ needs to be multiplied with the dimensionless Henry solubility of oxygen in the liquid (H) (Yang and Jensen, 2013).

$$D'_{O2,m} = D_{O2,m} \cdot H \qquad\qquad (26)$$

So, the oxygen diffusion coefficient in the membrane based on the oxygen concentration in the liquid phase would be one order of magnitude higher than the oxygen transverse dispersion coefficient or the oxygen effective diffusion coefficient in the catalyst particles. This resulted to the negligible effect on the reactant conversion when further decreasing the membrane thickness (e.g. enhancing the oxygen mass transfer in the membrane).
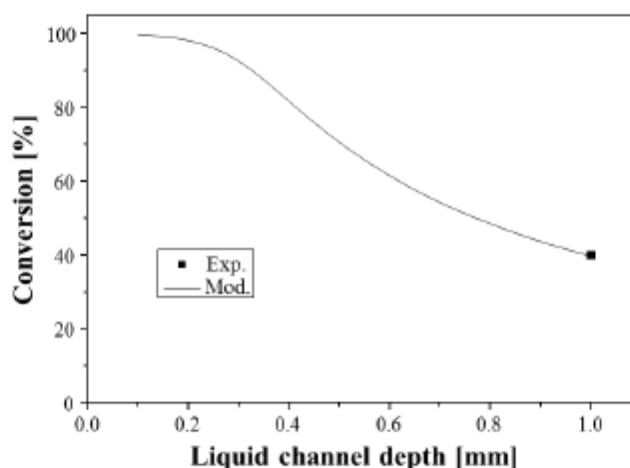
4.5 Effect of liquid channel depth

Figure 7. Effect of liquid channel depth on the conversion of benzyl alcohol, obtained from modelling. The square indicates experimental point. Reaction conditions: Ru/Al$_2$O$_3$ catalyst (90-125 μm), 10-100 mg; neat benzyl alcohol, 0.2-2 μL/min; catalyst contact time, 48 g$_{cat}$·min/g$_{BnOH}$; oxygen pressure, 8 bara; reaction temperature, 373 K.

Next, the effect of liquid channel depth on the conversion of benzyl alcohol was studied with constant catalyst contact time, and the results are shown in Figure 7. An approximately linear increase in conversion was observed when decreasing the liquid channel depth. At a liquid channel depth of 0.1 mm, the conversion reached 100%, which corresponded to a TOF of 26 h^{-1}. These results demonstrate a significant effect of the liquid channel depth on the conversion of benzyl alcohol and the TOF of the Ru/Al$_2$O$_3$ catalyst.

To better understand the effect of liquid channel depth, the concentration maps of benzyl alcohol and oxygen in the bulk liquid phase within the reactor are presented. For benzyl alcohol (shown in Figure 8), the bulk concentration decreased gradually along the axial direction, and at the same axial position, slightly lower concentration was observed in the catalyst bed close to the membrane. No obvious concentration difference was found between the bulk phase and the catalyst particle surface (see Figure 8c), as well as within the catalyst particle (see Figure S1 in the Supporting Information). However, oxygen was observed to exist only in a thin layer close to the membrane, and no oxygen was supplied in the main part of the catalyst bed (shown in Figure 9a). Specifically, the oxygen concentration at the same axial position dropped dramatically with y decreasing, and was equal to zero at y < 0.7 mm (see Figure 9b). Hence, the main part of the packed catalyst was unutilized resulting in low conversion and average TOF.

In Figure 9c, the oxygen concentrations in the bulk liquid are compared with those at the catalyst particle surface along the axial direction at different transverse positions. Only slight concentration difference ($\sim$0.8 mol/m^3, < 10% of the oxygen concentration in the bulk liquid phase), which was caused by the external mass transfer resistance, was observed at the catalyst bed close to the membrane (y = 0.95 mm) where relatively high concentration of oxygen existed. Since the external mass transfer was affected by the liquid flow rate and the TOF nearly stabilized at liquid flow rate > 2 μL/min (shown in Figure 4), it seems that the external mass transfer resistance does not influence the oxygen transfer in the membrane microchannel reactor.
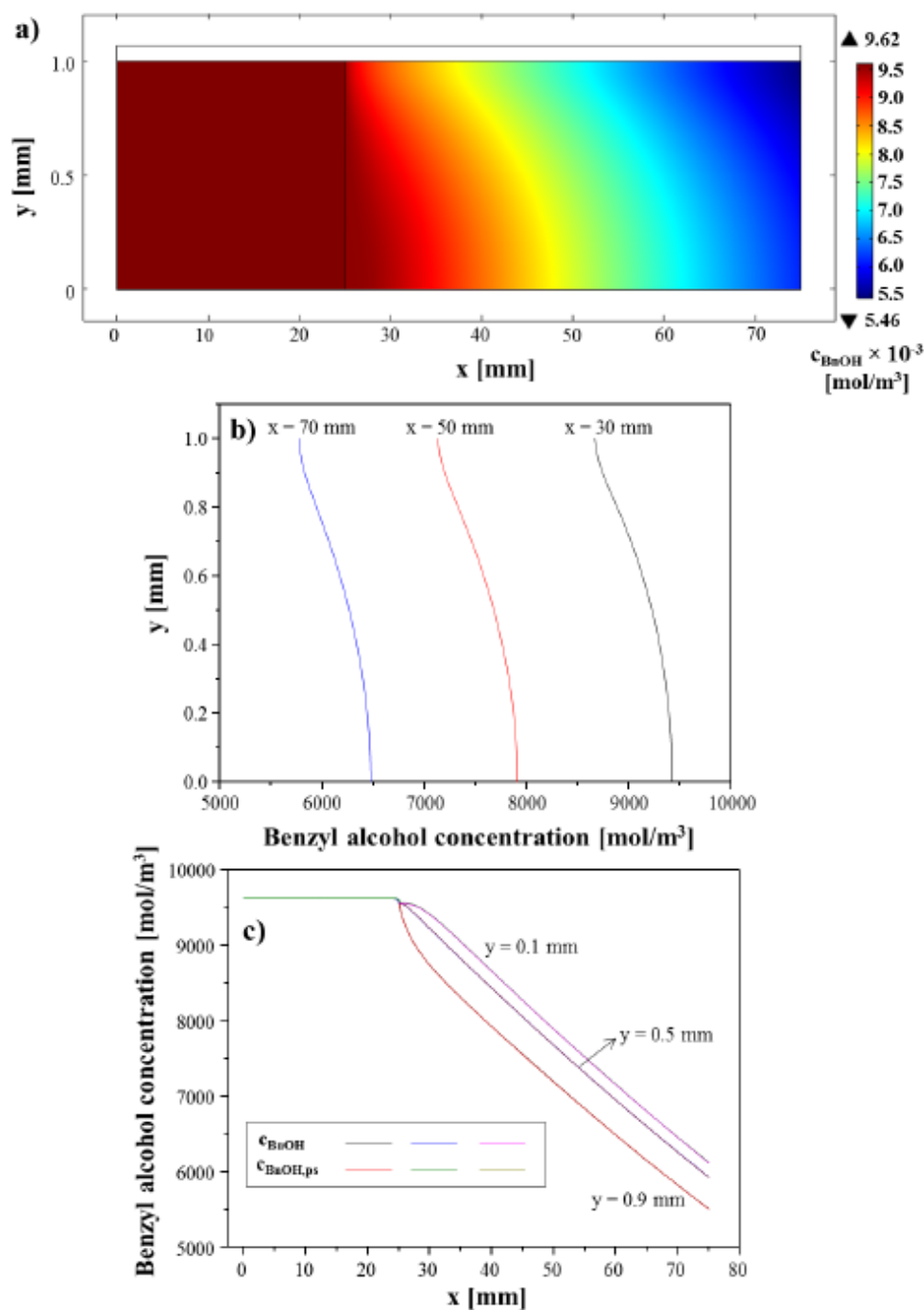
Figure 8. Benzyl alcohol concentration map and profiles in the bulk liquid phase within the reactor, obtained from modelling. a) Benzyl alcohol concentration map in the reactor, b) benzyl alcohol concentration profiles across the transverse direction at different axial positions, c) benzyl alcohol concentration profiles along the axial direction at different transverse positions. Reaction conditions: Ru/Al_2O_3 catalyst (90-125 μm), 100 mg; neat BnOH, 2 μL/min; catalyst contact time, 48 g_{cat}·min/g_{BnOH}; oxygen pressure, 8 bara; reaction

temperature, 373 K. c_{BnOH}: benzyl alcohol concentration in the bulk liquid, $c_{BnOH,ps}$: benzyl alcohol concentration at the catalyst particle surface.
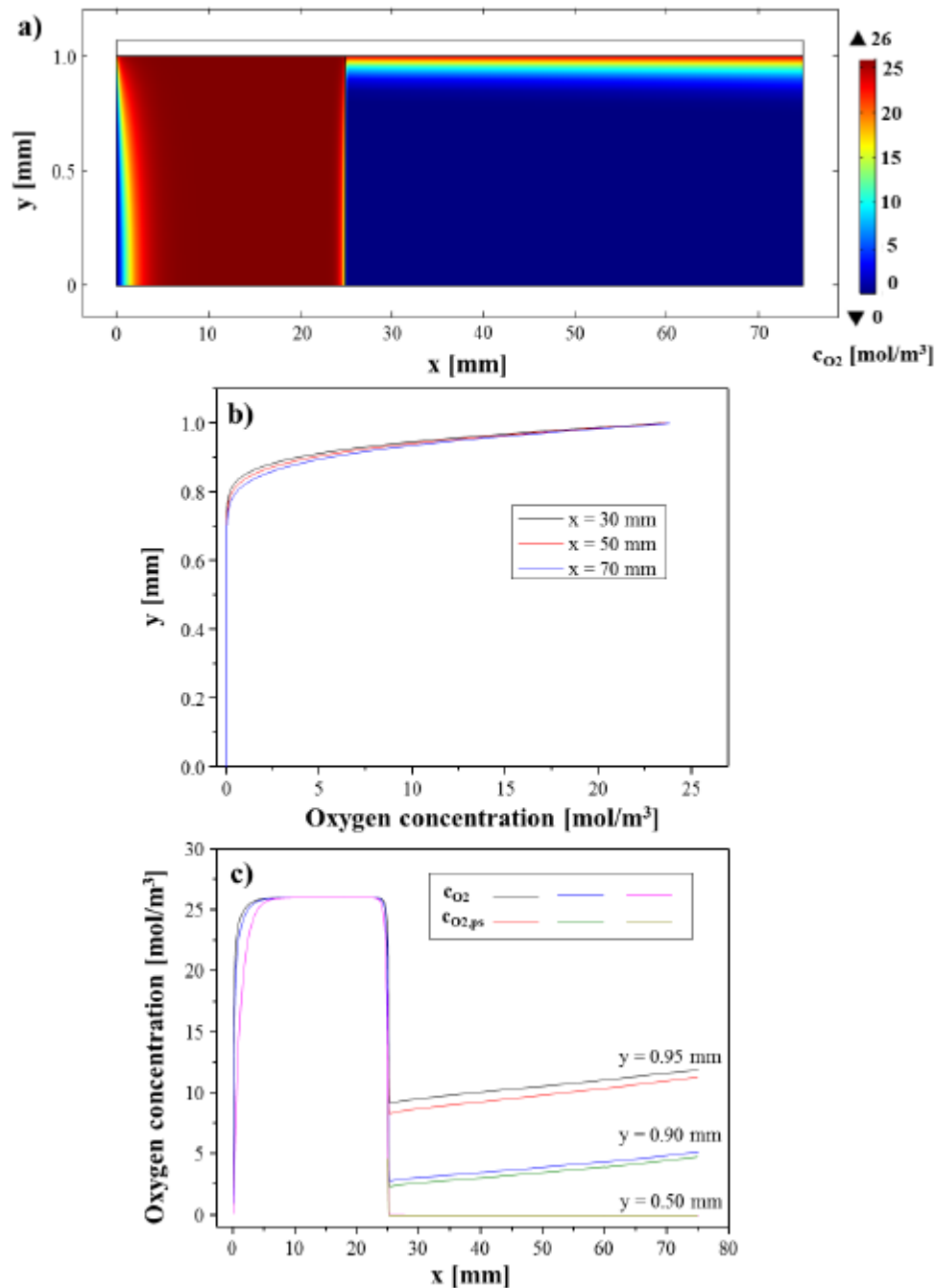

Figure 9. Oxygen concentration map and profiles in the bulk liquid phase within the reactor, obtained from modelling. a) Oxygen concentration map in the reactor, b) oxygen concentration profiles across the transverse direction at different axial positions, c) oxygen

concentration profiles along the axial direction at different transverse positions. Reaction conditions: Ru/Al$_2$O$_3$ catalyst (90-125 μm), 100 mg; neat BnOH, 2 μL/min; catalyst contact time, 48 g$_{cat}$·min/g$_{BnOH}$; oxygen pressure, 8 bara; reaction temperature, 373 K. c$_{O2}$: oxygen concentration in the bulk liquid, c$_{O2,ps}$: oxygen concentration at the catalyst particle surface.
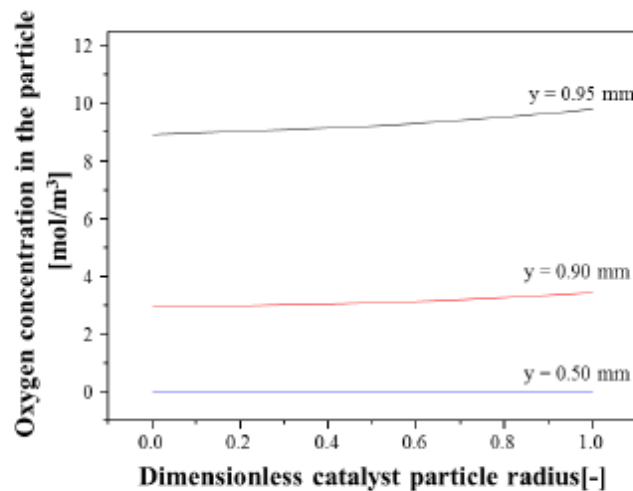

Figure 10. Oxygen concentration profiles in the catalyst particles at x = 50 mm, obtained from modelling. Reaction conditions: Ru/Al$_2$O$_3$ catalyst (90-125 μm), 100 mg; neat benzyl alcohol, 2 μL/min; catalyst contact time, 48 g$_{cat}$·min/g$_{BnOH}$; oxygen pressure, 8 bara; reaction temperature, 373 K.

The oxygen concentration profiles in the catalyst particles are presented in Figure 10. The concentration gradient in the catalyst particle, which was caused by the internal mass transfer resistance, was less than 10% of the oxygen concentration at the particle surface even for the particles close to the membrane (y = 0.95 mm). This was comparable to that caused by the external mass transfer resistance. When halving the particle size and assuming the same bed properties in the model, the conversion was observed to increase by only ~1 %, indicating negligible internal mass transfer resistance.

Note that in the laminar flow regime, the oxygen transfer in the packed bed of the membrane reactor includes transverse mass transfer through the bulk liquid in the catalyst bed, diffusion through the "stagnant film" at the catalyst particle surface and then within the catalyst particle pores. The liquid channel depth has presented a significant effect on the

reactant conversion in Figure 7. Since the external/internal mass transfer resistance in the membrane reactor had no obvious effect on the conversion, it seems that the significant effect of liquid channel depth is caused by the oxygen transverse mass transfer resistance in the catalyst bed. In the laminar flow regime, the oxygen transverse mass transfer rate is inversely proportional to the liquid channel depth, so an approximately linear increase in conversion was observed when decreasing the liquid channel depth. Halving the liquid channel depth from 1.0 to 0.5 mm led to conversion of benzyl alcohol increasing from 40% to 70% (see Figure 7). Correspondingly, the oxygen concentration in the catalyst bed was higher than zero at y > 0.2 mm (shown in Figure S2). These results suggest that the reactor performance could be improved through decreasing the liquid channel depth.

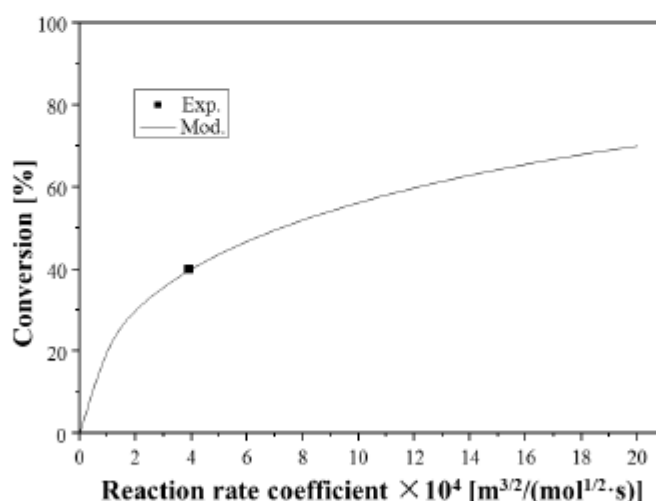4.6 Effect of reaction rate coefficient

Figure 11. Effect of reaction rate coefficient on the conversion of benzyl alcohol, obtained from experiment and modelling. Reaction conditions: Ru/Al_2O_3 catalyst (90-125 μm), 100 mg; neat benzyl alcohol, 2 μL/min; catalyst contact time, 48 $g_{cat} \cdot min/g_{BnOH}$; oxygen pressure, 8 bara; liquid pressure, 9.0 bara; reaction temperature, 373 K.

The effect of the reaction rate coefficient (k) on the conversion of benzyl alcohol was also investigated. From Figure 11, the conversion of benzyl alcohol was found to gradually rise

with k increasing, and reached 70% at $k = 2 \times 10^{-3}$ $m^{3/2}/(mol^{1/2} \cdot s)$. Since the oxygen consumed was supplied through the membrane, the gradual increase in the conversion indicates that the oxygen supply through the membrane could be enhanced at high reaction rate coefficient, due to the larger oxygen pressure difference across the membrane. However, the oxygen transverse mass transfer has been the controlling process with $k = 3.9 \times 10^{-4}$ $m^{3/2}/(mol^{1/2} \cdot s)$, further increasing the reaction rate coefficient would increase the oxygen demand by the catalyst, and thus cause more serious oxygen starvation in the catalyst bed and result to lower catalyst utilization. In order to fully utilize the catalyst packed in the membrane reactor, decreasing the reaction rate coefficient through decreasing the metal loading or choosing other less active catalyst can be considered. Alternatively, larger contribution of convective dispersion in the transverse direction in the catalyst bed could be induced by increasing the liquid velocity, in an attempt to enhance the transverse dispersion coefficient, at the expense of increasing pressure drop.

4. Conclusions

Aerobic oxidation of benzyl alcohol on Ru/Al_2O_3 catalyst was experimentally and theoretically investigated in a Teflon AF-2400 flat membrane microchannel reactor. The proposed model with the estimated kinetics was validated with the experimental data and provided a better understanding of the mass transfer and catalytic reactions in the membrane reactor. Transverse oxygen mass transfer, rather than the oxygen transfer in the membrane or the oxygen external/internal mass transfer, seems to be the controlling step for the membrane reactor performance for the system and conditions investigated. Correspondingly, decreasing the liquid channel depth is predicted to significantly increase the conversion and the average TOF of the catalyst. The conversion could also be increased by increasing the catalyst activity, but utilization of the highly active catalyst would be decreased due to the limitation

of the oxygen transverse mass transfer. To simultaneously improve the catalyst utilization and reactor conversion, the transverse dispersion coefficient should be increased, possibly by increasing the liquid velocity combined with recycling or using a forced convection mechanism (oscillation, ultrasonic vibration, etc.)

Acknowledgements

Nomenclature

A_b	active specific surface area in the 1D reactive catalyst bed [1/m]
CCT	catalyst contact time [$g_{cat} \cdot min/g_{BnOH}$]
c	concentration [mol/m^3]
d	depth [mm]
D	diffusion/dispersion coefficient [m^2/s]
Da	Damkohler number [-]
F	molar flow rate of alcohol [mol/min]
H	dimensionless Henry solubility [-]
h	mass transfer coefficient [m/s]
J	surface flux [$mol/(m^2 \cdot s)$]
k	reaction rate coefficient [$m^{3(\alpha+\beta-1)}/(mol^{(\alpha+\beta-1)} \cdot s)$]
l	length [mm]
M	molecular weight [g/mol]
m_{cat}	mass of catalyst [mg]
n_{Ru}	the moles of Ru contained in the catalyst packed [mol]
P	pressure [bara]

Pe	Peclet number [-]
r	radius [μm]
r_{dim}	spatial radial coordinate in the particle [μm]
$\bar{R}$	ideal gas constant [m^3·bar/(K·mol)]
R	reaction rate [mol/(m$^3_{bed}$·s)]
Re	particle Reynolds number [-]
S_B	selectivity to benzaldehyde [%]
Sc	Schmidt number [-]
Sh	Sherwood number [-]
T	temperature [K]
TOF	turnover frequency [h^{-1}]
u_x	axial liquid superficial velocity [cm/s]
w	width [mm]
X	conversion of benzyl alcohol [%]
x	x-coordinate [mm]
y	y-coordinate [mm]

Greek Symbols

α	reaction order in benzyl alcohol [-]
β	reaction order in oxygen [-]
ε	porosity or void fraction [-]
μ	viscosity [Pa·s]
ρ	density [g/mL]
υ	volumetric flow rate of benzyl alcohol [μL/min]

Subscripts

A	axial direction
B	benzaldehyde
BnOH	benzyl alcohol
b	catalyst bed
eff	effective diffusion coefficient in the catalyst
g	gas phase

i	benzyl alcohol, oxygen
in	inlet of the reactor
m	membrane
O_2	oxygen
out	outlet of the reactor
p	catalyst particle
ps	catalyst particle surface
T	transversal direction

References

Aran, H.C., Benito, S.P., Luiten-Olieman, M.W.J., Er, S., Wessling, M., Lefferts, L., Benes, N.E., Lammertink, R.G.H., 2011a. Carbon Nanofibers in Catalytic Membrane Microreactors. Journal of Membrane Science 381, 244-250.

Aran, H.C., Chinthaginjala, J.K., Groote, R., Roelofs, T., Lefferts, L., Wessling, M., Lammertink, R.G.H., 2011b. Porous Ceramic Mesoreactors: A New Approach for Gas-Liquid Contacting in Multiphase Microreaction Technology. Chemical Engineering Journal 169, 239-246.

Bavykin, D.V., Lapkin, A.A., Kolaczkowski, S.T., Plucinski, P.K., 2005. Selective Oxidation of Alcohols in a Continuous Multifunctional Reactor: Ruthenium Oxide Catalysed Oxidation of Benzyl Alcohol. Applied Catalysis A: General 288, 175-184.

Brazier, J.B., Hellgardt, K., Hii, K.K., 2017. Catalysis in Flow: O_2 Effect on the Catalytic Activity of $Ru(OH)_x/\gamma$ -Al_2O_3 during the Aerobic Oxidation of an Alcohol. Reaction Chemistry & Engineering 2, 60-67.

Brzozowski, M., O'Brien, M., Ley, S.V., Polyzos, A., 2015. Flow Chemistry: Intelligent Processing of Gas–Liquid Transformations Using a Tube-in-Tube Reactor. Accounts of Chemical Research 48, 349-362.

Constantinou, A., Wu, G., Corredera, A., Ellis, P., Bethell, D., Hutchings, G.J., Kuhn, S., Gavriilidis, A., 2015. Continuous Heterogeneously Catalyzed Oxidation of Benzyl Alcohol in a Ceramic Membrane Packed-Bed Reactor. Organic Process Research & Development 19, 1973-1979.

Davis, S.E., Ide, M.S., Davis, R.J., 2013. Selective Oxidation of Alcohols and Aldehydes over Supported Metal Nanoparticles. Green Chemistry 15, 17-45.

Delgado, J.M.P.Q., 2006. A Critical Review of Dispersion in Packed Beds. Heat and Mass Transfer 42, 279-310.

Elvira, K.S., i Solvas, X.C., Wootton, R.C.R., deMello, A.J., 2013. The Past, Present and Potential for Microfluidic Reactor Technology in Chemical Synthesis. Nat Chem 5, 905-915.

Froessling, N., 1938. Über die verdunstung fallender tropfen. Gerlands Beiträge zur Geophysik 52, 170-215.

Froment, G.F., Bischoff, K.B., De Wilde, J., 2010. Chemical Reactor Analysis and Design, 3rd Edition. John Wiley & Sons, Incorporated, United States of America.

Gavriilidis, A., Constantinou, A., Hellgardt, K., Hii, K.K., Hutchings, G.J., Brett, G.L., Kuhn, S., Marsden, S.P., 2016. Aerobic Oxidations in Flow: Opportunities for the Fine Chemicals and Pharmaceuticals Industries. Reaction Chemistry & Engineering 1, 595-612.

Gemoets, H.P.L., Su, Y., Shang, M., Hessel, V., Luque, R., Noel, T., 2016. Liquid Phase Oxidation Chemistry in Continuous-Flow Microreactors. Chemical Society Reviews 45, 83-117.

Goethals, M., Vanderstraeten, B., Berghmans, J., De Smedt, G., Vliegen, S., Van't Oost, E., 1999. Experimental Study of the Flammability Limits of Toluene–Air Mixtures at Elevated Pressure and Temperature. Journal of Hazardous Materials 70, 93-104.

Greene, J.F., Preger, Y., Stahl, S.S., Root, T.W., 2015. PTFE-Membrane Flow Reactor for Aerobic Oxidation Reactions and Its Application to Alcohol Oxidation. Organic Process Research & Development 19, 858-864.

Gutmann, B., Cantillo, D., Kappe, C.O., 2015. Continuous-Flow Technology—A Tool for the Safe Manufacturing of Active Pharmaceutical Ingredients. Angewandte Chemie International Edition 54, 6688-6728.

Hayduk, W., Buckley, W.D., 1972. Effect of Molecular Size and Shape on Diffusivity in Dilute Liquid Solutions. Chemical Engineering Science 27, 1997-2003.

Hessel, V., Angeli, P., Gavriilidis, A., Löwe, H., 2005. Gas–Liquid and Gas–Liquid–Solid Microstructured Reactors: Contacting Principles and Applications. Industrial & Engineering Chemistry Research 44, 9750-9769.

Hogg, S.R., Muthu, S., O'Callaghan, M., Lahitte, J.-F., Bruening, M.L., 2012. Wet Air Oxidation of Formic Acid Using Nanoparticle-Modified Polysulfone Hollow Fibers as Gas–Liquid Contactors. ACS Applied Materials & Interfaces 4, 1440-1448.

Hone, C.A., Roberge, D.M., Kappe, C.O., 2017. The Use of Molecular Oxygen in Pharmaceutical Manufacturing: Is Flow the Way to Go? ChemSusChem 10, 32-41.

Jähnisch, K., Hessel, V., Löwe, H., Baerns, M., 2004. Chemistry in Microstructured Reactors. Angewandte Chemie International Edition 43, 406-446.

Liu, M., Zhu, X., Chen, R., Liao, Q., Feng, H., Li, L., 2016. Catalytic Membrane Microreactor with Pd/γ -Al_2O_3 Coated PDMS Film Modified by Dopamine for Hydrogenation of Nitrobenzene. Chemical Engineering Journal 301, 35-41.

Mallat, T., Baiker, A., 2004. Oxidation of Alcohols with Molecular Oxygen on Solid Catalysts. Chemical Reviews 104, 3037-3058.

Mallia, C.J., Baxendale, I.R., 2015. The Use of Gases in Flow Synthesis. Organic Process Research & Development 20, 327-360.

Mannel, D.S., Stahl, S.S., Root, T.W., 2014. Continuous Flow Aerobic Alcohol Oxidation Reactions Using a Heterogeneous $Ru(OH)_x/Al_2O_3$ Catalyst. Organic Process Research & Development 18, 1503-1508.

Mo, Y., Imbrogno, J., Zhang, H., Jensen, K.F., 2018. Scalable thin-layer membrane reactor for heterogeneous and homogeneous catalytic gas–liquid reactions. Green Chemistry 20, 3867-3874.

Nayar, S., Kudchadker, A.P., 1973. Densities of Some Organic Substances. Journal of Chemical & Engineering Data 18, 356-357.

Noël, T., Hessel, V., 2013. Membrane Microreactors: Gas–Liquid Reactions Made Easy. ChemSusChem 6, 405-407.

Pieber, B., Kappe, C.O., 2016. Aerobic Oxidations in Continuous Flow, in: Noël, T. (Ed.), Organometallic Flow Chemistry. Springer Berlin Heidelberg, Cham, pp. 97-136.

Reddy, K.A., Doraiswamy, L.K., 1967. Estimating Liquid Diffusivity. Industrial & Engineering Chemistry Fundamentals 6, 77-79.

Richardson, J.F., Harker, J.H., Backhurst, J.R., 2002. CHAPTER 4 - Flow of Fluids through Granular Beds and Packed Columns, Chemical Engineering (Fifth Edition). Butterworth-Heinemann, Oxford, pp. 191-236.

Selinsek, M., Bohrer, M., Vankayala, B.K., Haas-Santo, K., Kraut, M., Dittmeyer, R., 2016. Towards a New Membrane Micro Reactor System for Direct Synthesis of Hydrogen Peroxide. Catalysis Today 268, 85-94.

Tan, X., Li, K., 2013. Membrane Microreactors for Catalytic Reactions. Journal of Chemical Technology & Biotechnology 88, 1771-1779.

Wilke, C.R., Chang, P., 1955. Correlation of Diffusion Coefficients in Dilute Solutions. AIChE Journal 1, 264-270.

Wu, G., Cao, E., Kuhn, S., Gavriilidis, A., 2017. A Novel Approach for Measuring Gas Solubility Using a Tube-in-Tube Membrane Contactor. Chemical Engineering & Technology 40, 2346-2350.

Wu, G., Constantinou, A., Cao, E., Kuhn, S., Morad, M., Sankar, M., Bethell, D., Hutchings, G.J., Gavriilidis, A., 2015. Continuous Heterogeneously Catalyzed Oxidation of Benzyl Alcohol Using a Tube-in-Tube Membrane Microreactor. Industrial & Engineering Chemistry Research 54, 4183-4189.

Yamaguchi, K., Mizuno, N., 2002. Supported Ruthenium Catalyst for the Heterogeneous Oxidation of Alcohols with Molecular Oxygen. Angewandte Chemie International Edition 41, 4538-4542.

Yamaguchi, K., Mizuno, N., 2003. Scope, Kinetics, and Mechanistic Aspects of Aerobic Oxidations Catalyzed by Ruthenium Supported on Alumina. Chemistry – A European Journal 9, 4353-4361.

Yang, L., Jensen, K.F., 2013. Mass Transport and Reactions in the Tube-in-Tube Reactor. Organic Process Research & Development 17, 927-933.

Yang, Z.-W., Zhao, X., Li, T.-J., Chen, W.-L., Kang, Q.-X., Xu, X.-Q., Liang, X.-X., Feng, Y., Duan, H.-H., Lei, Z.-Q., 2015. Catalytic Properties of Palygorskite Supported Ru and Pd for Efficient Oxidation of Alcohols. Catalysis Communications 65, 34-40.

Yaws, C.L., 2014. Chapter 3 - Viscosity of Liquid – Organic Compounds, Transport Properties of Chemicals and Hydrocarbons (Second Edition). Gulf Publishing Company, Oxford, pp. 131-254.

Zhang, H., Weber, S.G., 2012. Teflon AF Materials, in: Horvath, I.T. (Ed.), Fluorous Chemistry. Springer-Verlag Berlin, Berlin, pp. 307-337.

Zotova, N., Hellgardt, K., Kelsall, G.H., Jessiman, A.S., Hii, K.K., 2010. Catalysis in Flow: the Practical and Selective Aerobic Oxidation of Alcohols to Aldehydes and Ketones. Green Chemistry 12, 2157-2163.